Journal of the European Ceramic Society 9 (1992) 417–425

Influence of Chemical Composition on Corrosion of Alumina in Acids and Caustic Solutions

W. Genthe & H. Hausner

Technische Universität Berlin, Institut für Nichtmetallische Werkstoffe, Englische Strasse 20, 1000 Berlin 12, FRG

(Received 13 June 1991; revised version received 7 October 1991; accepted 14 October 1991)

Abstract

The corrosion behaviour of pure alumina, doped with different amounts of MgO, Y_2O_3, ZrO_2, Cr_2O_3, Co_3O_4 and BaO, was investigated. Corrosion media were concentrated HCl, HNO_3, HF, H_2SO_4/H_3PO_4 (1:1 mixture), HCl (1%) and NaOH (10%). The reaction conditions were 180°C (autoclave) for 168 h. The corroded specimens were investigated by SEM, the leaching solutions were analysed with ICP-OES (optical emission spectroscopy with inductively coupled plasma). The corrosion resistance was found to depend mainly on the microstructure and the composition of the grain boundary phase. Both parameters are influenced by the type and concentration of the additive, the method by which the sintering aid was added and the sintering conditions.

Reines Aluminiumoxid wurde mit verschiedenen Mengen MgO, Y_2O_3, ZrO_2, Cr_2O_3, Co_3O_4 und BaO dotiert, gesintert und einem Korrosionstest unterzogen. Als Korrosionsmedien wurden konzentrierte HCl, HNO_3, HF, H_2SO_4/H_3PO_4 (1:1 Mischung), HCl (1%) und NaOH (10%) verwendet. Die Reaktionsbedingungen waren 180°C während 168 Stunden unter Eigendruck im Autoclaven. Die korrodierten Probekörper wurden mit REM, die Leachinglösungen mit ICP-OES (optical emission spectroscopy with inductively coupled plasma)untersucht. 'Der jeweils ermittelte Korrosionswiderstand hängt überwiegend von der Ausbildung des Gefüges und der Zusammensetzung der Korngrenzphase ab; beide Parameter werden durch die Art, Menge und die Einbringung des Additivs und die Sinterbedingen beeinflußt.

De l'oxyde d'aluminium pur additionné de divers quantités de MgO, Y_2O_3, ZrO_2, Cr_2O_3, Co_3O_4 et BaO a été fritté et soumis à un test de corrosion. Les agents de corrosion, HCl, HNO_3, HF, H_2SO_4/H_3PO_4 (en solution de 1 pour 1) concentrès, une solution de HCl à 1% et une solution de NaOH à 10% ont été utilisés avec les conditions de réaction suivantes: 180°C, pendant 168 heures sous pression en autoclave. Les éprouvettes corrodées ont été étudiées au REM, la 'leaching' solution à l' ICP-OES (optical emission spectroscopy with inductively coupled plasma). Pour chacune, le calcul de la résistance à la corrosion montre que celle-ci dèpend essentiellement de la formation de la microstructure et de la composition du joint de grain. Ces deux paramétres sont influencès par la nature, la quantité et l'ajout d'additif ainsi que par les conditions de frittage.

1 Introduction

Although in general ceramics have a high resistance against corrosion, they can be attacked under certain conditions when they are in contact with corrosive liquids. Published results in this area are limited, e.g. Refs 1–5. In an earlier work[6] the present authors showed the behaviour of commercially available aluminium oxide ceramics including transparent alumina and the influence of different amounts of silica in aluminium oxide on the corrosion behaviour in inorganic acids.[7] In addition the influence of grain boundaries on the corrosion resistance of aluminas[8] and the corrosion behaviour of other ceramics, e.g. ZrO_2[9] and SiC/TiC,[10] were investigated.

2 Experimental Procedure

2.1 Preparation of specimens

The additives were prepared as coprecipitates of the corresponding metal nitrates and aluminium nitrate

Journal of the European Ceramic Society 0955-2219/92/$5.00

Table 1. Sintering conditions, additive concentration (μg/g), density and grain size of sintered specimens

Sample	*Sintering temperature* T_{max}(°C)	*Time at* T_{max} (*h*)	*Additive* (μg/g)	*Sintered density* (% *th. d.*)	*Grain size* (μm)
5 Ba	1550	4	700 Ba	98·35	2·6
25 Ba	1550	4	2030 Ba	96·92	2·1
100 Ba	1550	4	6750 Ba	95·56	2·9
5 Co	1550	5	280 Co	96·64	2·1
25 Co	1550	3	900 Co	97·42	3·1
5 Cr	1550	3	91 Cr	95·94	2·3
25 Cr	1550	4	1142 Cr	96·87	2·1
100 Cr	1550	4	4330 Cr	97·01	2·8
5 Mg	1550	4	190 Mg	97·77	3·0
5 Mg1	1600	4	180 Mg	99·27	5·4
25 Mg	1550	4	1300 Mg	96·01	2·5
100 Mg2	1500	4	5470 Mg	95·06	2·1
100 Mg	1550	4	5310 Mg	96·66	2·3
100 Mg1	1600	4	5560 Mg	97·49	2·6
5 Y	1550	5	213 Y	97·76	2·6
5 Y1	1600	4	208 Y	97·57	5·4
10 Y	1550	4	429 Y	97·58	4·2
25 Y	1550	3	2043 Y	96·75	3·5
25 Y1	1600	4	1931 Y	97·90	4·2
50 Y	1550	4	3022 Y	95·80	2·6
100 Y	1550	4	4230 Y	97·18	4·2
100 Y1	1600	4	4026 Y	97·43	4·4
5 Zr	1550	4	930 Zr	97·95	2·6
25 Zr	1550	3	4540 Zr	97·15	2·0
100 Zr	1550	3	15260 Zr	95·16	3·8

at 70°C with aqueous ammonia solution in a Teflon beaker. The hydroxide mixtures were washed with ammonia solution until the washing solution contained less than 100 mg/litre NO_3^-. After freeze-drying, 120 g alumina (AKP 50, Sumitomo) in 500 ml demineralised water was added and the mixture was homogenised in a ball mill (ZrO_2 beads). After homogenisation the slurry was freeze-dried. The exact concentration of the additives was determined by ICP-OES and is shown in Table 1.

After addition of 5% isopropanol the mixtures were granulated and compacted with a pressure of 100 KN to plates of 60 × 60 × 8 mm. The green bodies with an average density of 2·17 g/cm^3 were dried for 24 h at 120°C and sintered in a platinum vessel. The sintering conditions, which have not been optimised for each composition, are shown in Table 1. The test specimens were cut from the sintered plates and polished to a roughness of 1 μm.

2.2 Corrosion testing

The specimens with a weight of approximately 1 g each were corrosion tested in concentrated hydrochloric acid, hydrofluoric acid, nitric acid, a 1:1 mixture of sulphuric and phosphoric acid, 1% hydrochloric acid, and 10% caustic soda solution (all Suprapur, Merck, Darmstadt, FRG). The corrosion experiments were carried out in 50 ml Teflon-lined autoclaves (Berghof, Eningen, FRG). The concentrations are shown in Table 2.

After the corrosion test, the individual specimens were washed several times with deionised water, dried for 1 h at 120°C and investigated by SEM. The leaching solution was added to the washing solution, filled up to 100 ml and analysed by ICP-OES.

2.3 Analytical method

A sequential ICP spectrometer (ARL 3520) with a corrosion resistant atomising system was used[6,7] to analyse the chemical compositions of all raw materials, ceramics and leaching solutions. The calibration standards were prepared by dilution of 1000 ppm standards (Merck and Alfa Ventron, Karlsruhe, FRG). The spectral lines used for analysis are listed in Table 3.

Table 2. Corrosion conditions

Corrosive medium	*Temperature* (°C)	*Time* (*h*)
HCl, 30%	180	168
HNO_3, 65%	180	168
HF, 35%	180	168
H_2SO_4 (96%)/H_3PO_4 (85%) 1:1	180	168
HCl, 1%	245	24
NaOH	180	168
NaOH	215	168

Table 3. Analytical lines for spectrochemical analysis

Element	*Wavelength*	*Type of spectral line*	*Order*	*Position of background correction (nm)*
Al	308·215	I	2	+0·06
Cr	267·716	II	2	−0·08
Mg	279·080	II	2	−0·05
Y	371·030	II	2	+0·1
Ba	455·403	II	1	−0·1
Na	589·592	I	1	+0·1
Ca	393·366	II	2	−0·1
Fe	259·940	II	2	+0·1
Ti	337·280	II	2	−0·1
K	766·490	I	1	±0·1
Ni	231·604	II	2	+0·06
Mn	257·610	II	2	+0·1
Pt	265·945	I	2	−0·03
Si	251·611	I	2	−0·08
Sn	235·484	I	2	—

The SE micrographs were obtained using a Cambridge Stereoscan 180; the specimens were sputtered with a 1·5 μm layer of gold.

3 Composition of Materials

The AKP 50 powder has impurities of Si, Na, Mg, Cu and Fe with a concentration of each element lower than 10 μg/g, a specific surface of 12 m^2/g and a grain size between 0·1 and 0·3 μm. The powder mixtures were characterised by dilatometry and dL/L_0 and dL/dt_{max} curves were recorded. dL/dt_{max} was found to be between 1300°C and 1400°C.

The mean compositions of the specimens are shown in Table 1. The impurity concentration of the sintered specimens increased slightly during preparation. However, the amount of Ca and Na is still lower than 50 μg/g; Mg and Si lower than 30 μg/g; and Fe lower than 20 μg/g; other impurity concentrations like B and Ti are in the order of 10 μg/g or less.

The apparent density of the ceramic specimens was determined by the buoyancy method. The microstructure was analysed by optical or scanning electron microscopy according to DIN standard 50601 and ASTM standard 112-77. Some of the samples showed discontinuous grain growth. The results of these measurements are shown in Table 1.

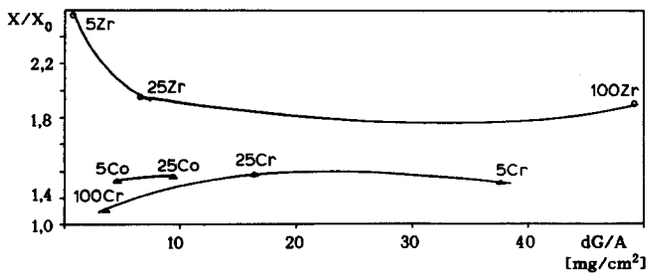

Fig. 1. Specific weight loss and ratio of additive concentration in leaching solutions and bulk material ($HCl_{conc.}$, 180°C and 168 h); (○) zirconium oxide-doped alumina, (△) cobalt oxide-doped alumina and (▲) chromium oxide-doped alumina.

4 Results and Discussion

In Fig. 1 the results of the corrosion experiments in concentrated HCl with the ZrO_2-, Co_3O_4-, and Cr_2O_3-doped samples are shown. The relative weight loss, dG/A, is plotted against the relative concentration of the additive element in the leaching solution (this number equals 1 if the concentration

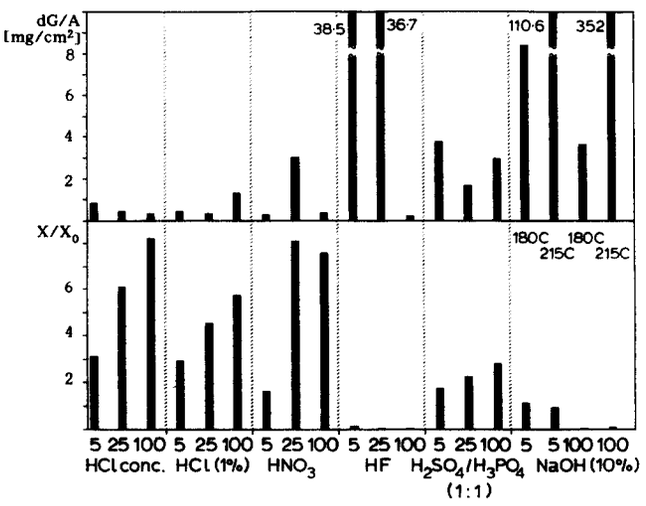

Fig. 2. Specific weight loss and ratio of additive concentration in leaching solutions and bulk material of MgO-doped samples. Corrosion conditions: 180°C, 168 h (if not indicated differently). In the case of 1% HCl: 245°C, 24 h. Sintering temperature for 5 Mg1, 25 Mg1 and 100 Mg1 samples: 1600°C.

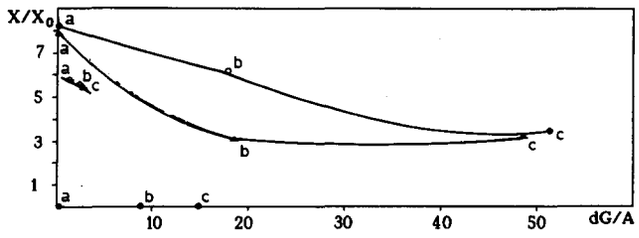

Fig. 3. Specific weight loss and ratio of additive concentration in leaching solutions and bulk material of a MgO-doped alumina (5500 μg/g Mg) sintered at different temperatures: (a) 1600°C; (b) 1550°C; (c) 1500°C; (○) $HCl_{conc.}$, 180°C, 168 h; (▲) HNO_3, 180°C, 168 h; (△) HCl (1%), 245°C, 24 h; (●) HF; 180°C, 168 h.

of the element in the leaching solution is identical to the concentration in the bulk ceramic). These two parameters are a good indication for the corrosion behaviour.

The relative weight loss characterises the total corrosion resistance of the specimens. It correlates well with the aluminium concentration of the leaching solution. Only in those cases where solid reaction products have been formed on the surface of the specimens or where diffusion of corrosion media into the specimen has occurred is no correlation observed. Especially in the case of very

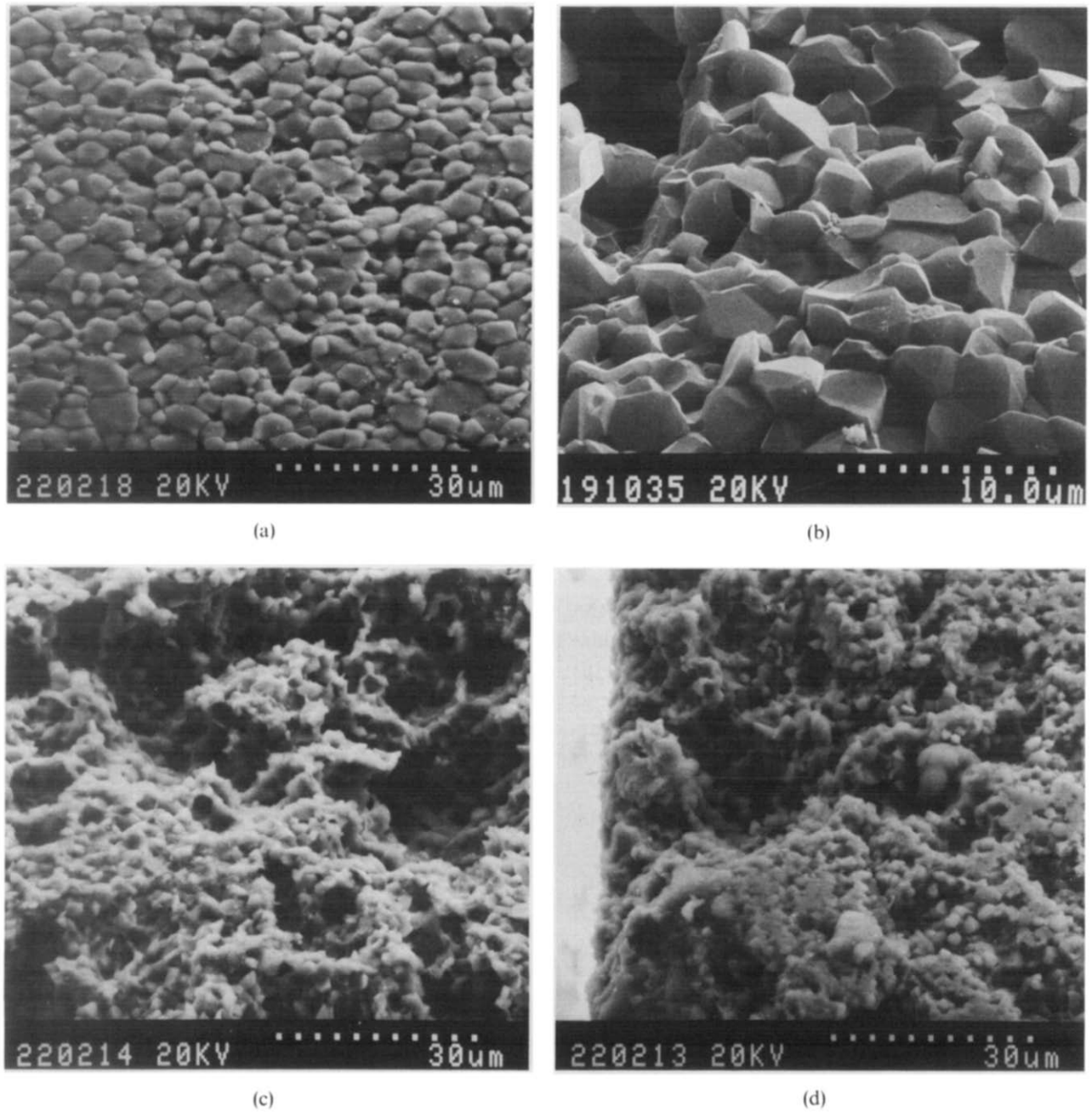

Fig. 4. SEM micrographs of samples (100 Mg1, 100 Mg and 100 Mg2) which have been sintered at different temperatures after a corrosion experiment in $HCl_{conc.}$ (180°C, 168 h). (a) $T_{max} = 1600$°C (surface); (b) $T_{max} = 1550$°C (surface); (c) $T_{max} = 1500$°C (surface); (d) $T_{max} = 1500$°C (cross-section).

high corrosion resistance a weight gain of the specimens can be observed. In these cases it would be more appropriate to plot the aluminium concentrations of the leaching solutions. Nevertheless, consideration of the relative weight loss is sufficient in most cases.

The relative concentration of the additive in the leaching solution is an indication for the possible formation of a grain boundary phase, and its chemical stability. In the case of zirconium and cobalt oxide additions corrosion resistance decreases with additive concentration, while in the case of the chromium oxide-doped alumina the opposite is observed. The relative additive concentration in the leaching solution is higher for zirconium oxide-doped aluminas than for the chromium oxide-doped aluminas, i.e. zirconium oxide is leached out more on a relative basis. These phenomena can be caused by a higher concentration of zirconium oxide in the grain boundary phase and the solid solution of chromium oxide in alumina.

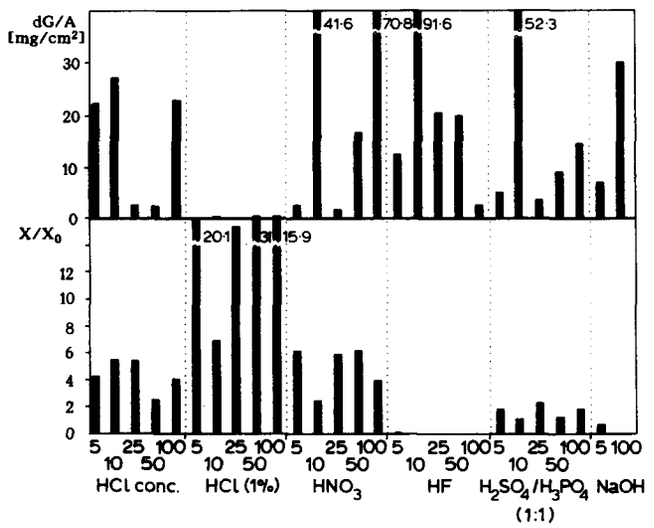

Fig. 5. Specific weight loss and ratio of additive concentration in leaching solutions and bulk material for Y_2O_3-doped alumina. Corrosion results with samples 5 Y, 10 Y, 25 Y, 50 Y and 100 Y, sintered at 1550°C in concentrated HCl, HNO_3, HF, H_2SO_4/H_3PO_4 (1:1) and NaOH (10%) at 180°C, 168 h and HCl (1%) at 245°C, 24 h.

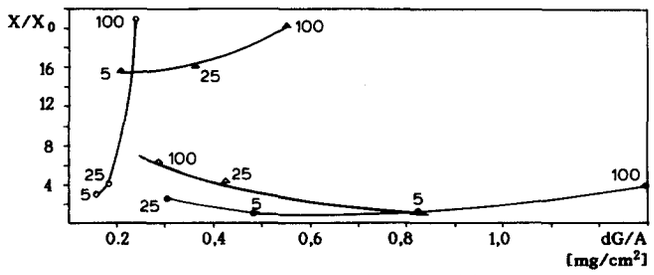

Fig. 6. Specific weight loss and ratio of additive concentration in leaching solutions and bulk material of Y_2O_3- and MgO-doped alumina sintered at 1600°C. (○) Y_2O_3-doped samples (5 Y1, 25 Y1, 100 Y1) in $HCl_{conc.}$ (180°C, 168 h); (▲) Y_2O_3-doped samples (5 Y1, 25 Y1, 100 Y1) in HCl (1%) (245°C, 24 h); (△) MgO-doped samples (5 Mg1, 25 Mg1, 100 Mg1) in $HCl_{conc.}$ (180°C, 168 h); (●) MgO-doped samples (5 Mg1, 25 Mg1, 100 Mg1) in HCl (1%) (245°C, 24 h).

4.1 MgO-Doped alumina

The magnesium oxide-doped aluminas, which have been sintered at 1600°C, show a good corrosion resistance except in concentrated HF and NaOH (Fig. 2). In HF only the highly doped sample (100 Mg1) is fairly resistant. Caustic soda causes total dissolution, especially at high temperatures (215°C). The low magnesium concentrations in the leaching solutions are caused by the low solubility of the magnesium compounds in these solutions.

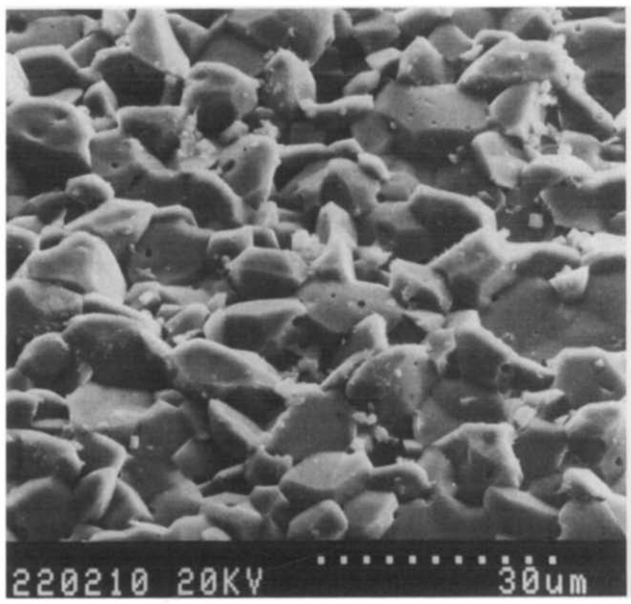

(a)

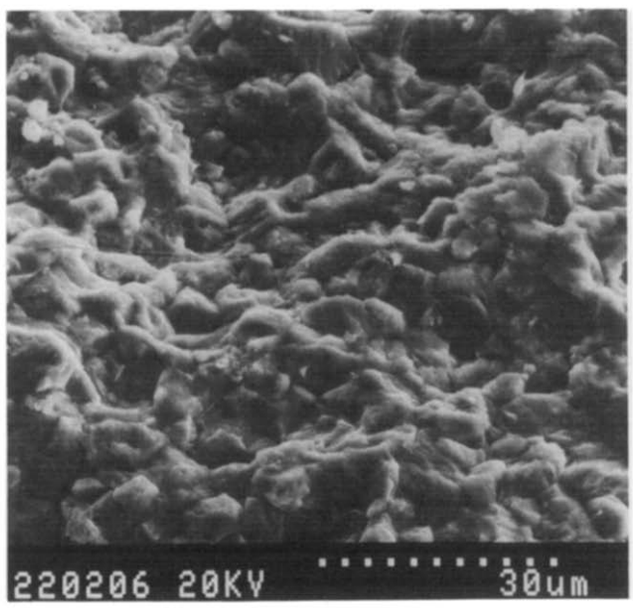

(b)

Fig. 7. SEM micrographs of a Y_2O_3-doped sample (5 Y1) sintered at 1600°C, after corrosion experiments (180°C, 168 h) in (a) HF (surface) and (b) HNO_3 (surface).

The influence of sintering temperature on corrosion resistance is very strong as is shown for one magnesium oxide concentration in Fig. 3. The specimens react similarly in concentrated HCl and HNO_3; with decreasing sintering temperature the corrosion resistance also decreases drastically. Also the relative magnesium concentration in the leaching solution is decreased; this result seems to indicate that the attack is more homogeneous. In the experiments with diluted HCl the situation seems to be different: due to the short reaction time and the higher reaction temperature a preferred attack can be observed and the influence of sintering temperature is less pronounced. In the HF-corroded specimens Mg is not detectable in the leaching solutions because of the insolubility of MgF_2. Compared to the results of experiments with HCl or HNO_3 the influence of sintering temperature is lower, which can be explained by the fact that the diffusion is retarded by the insoluble AlF_3 and MgF_2. Experiments with a 1:1 mixture of H_2SO_4 and H_3PO_4 resulted in a strong attack of the samples which were sintered at low temperature ($dG/A = 218\,mg/cm^2$ for $T_{sint.} = 1500°C$ and $dG/A = 135\,mg/cm^2$ for $T_{sint.} = 1550°C$). In Fig. 4 scanning electron micrographs of experiments with concentrated HCl are shown. The heavily attacked surface of the $T_{max} = 1500°C$ sample is shown, whereas the surface of the $T_{max} = 1600°C$ sample is rather intact. EDX analysis of the $T_{max} = 1500°C$ sample showed a lower magnesium concentration at the outer part of the sample in comparison with the centre section.

For the different behaviour of the samples the different porosity seems to be the most obvious factor, but also the composition of the grain boundary phase, which may change with sintering temperatures, is very important.

4.2 Y_2O_3-Doped alumina

In Fig. 5, the experiments with yttrium oxide-doped aluminas, sintered at 1550°C, are shown. In comparison with samples sintered at 1600°C (see below) the corrosive attack is stronger. Only the samples 25Y and 50Y have a fairly good resistance. Remarkable is the strong influence of concentration with all specimens corroded in HCl. A much higher corrosion resistance has been obtained with samples sintered at 1600°C. Figure 6 shows that the decrease in corrosion resistance with additive concentration is small in concentrated HCl at 180°C and higher in 1% HCl at 245°C. This result shows that temperature has a stronger influence on corrosion than acid concentration. The relative yttrium concentrations in the leaching solutions are high and increase with the amount of additive concentration in the aluminas. In Fig. 6 the corrosion of magnesium oxide-doped samples sintered at 1600°C in concentrated and diluted HCl is also shown. The corrosion resistance as well as the relative magnesium concentration of the leaching solutions is lower than in the case of Y_2O_3-doped material.

The alumina with low Y_2O_3 content has a weight loss of $0{\cdot}16\,mg/cm^2$ after one week in concentrated HCl at 180°C. This corresponds to a corrosion resistance which is close to the resistance

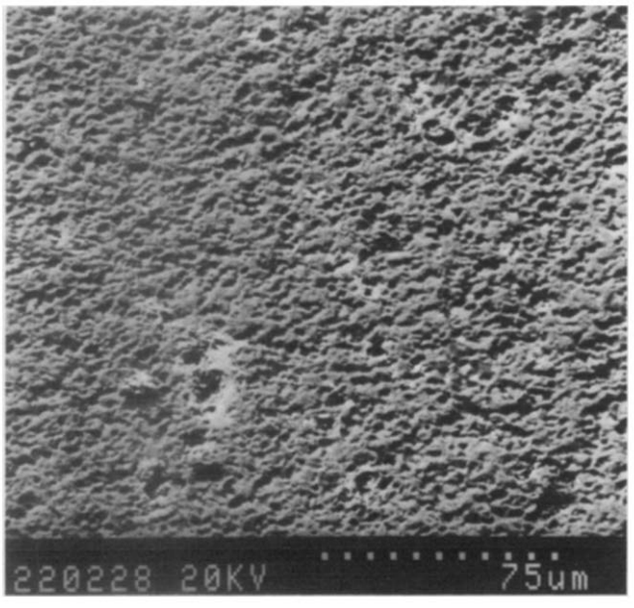

Fig. 8. SEM micrograph of a BaO-doped alumina (100 Ba) after a corrosion experiment in $HCl_{conc.}$ (180°C, 168 h); backscattered electrons.

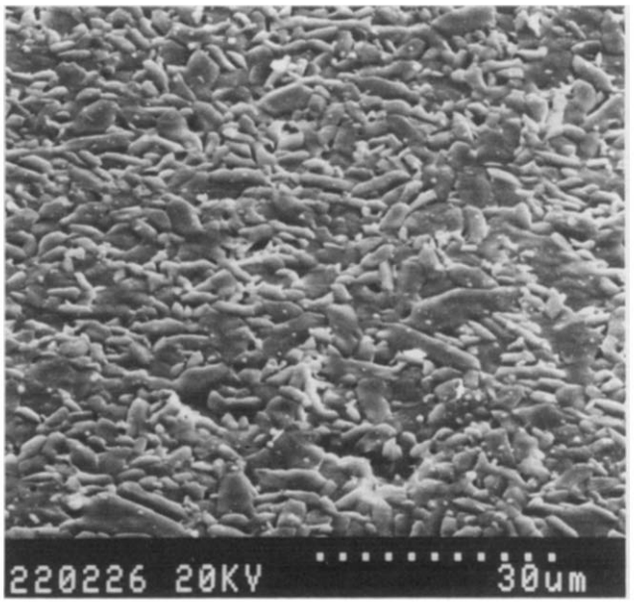

Fig. 9. SEM micrograph of a BaO-doped alumina (25 Ba) after a corrosion experiment in $HCl_{conc.}$ (180°C, 168 h).

of single crystal aluminum oxide. In concentrated HF the resistance is lower. In Fig. 7 the surface of Y_2O_3-doped samples is shown after the corrosion test. Beside reaction products the attack of the grains can be seen.

4.3 BaO-Doped alumina

Figure 8 shows a scanning electron micrograph (backscattered electrons) of the 100 Ba sample. The dark points are caused by the barium oxide, which has formed a new phase. Figure 9 shows the surface of another barium oxide-doped alumina after the corrosive attack of concentrated HCl at 180°C for one week. The barium oxide-doped aluminas are the only specimens in the series with elongated grains. In concentrated HCl a special corrosion mechanism seems to exist for the barium oxide-doped aluminas: the relative barium concentration in the leaching solutions is very high ($Ba/Ba_0 = 71{\cdot}9$ for the 5 Ba sample, 27·9 for 25 Ba and 13·1 for 100 Ba).

In Fig. 10 the experiments with barium oxide-doped alumina are shown. In all corrosion media the resistance decreases with the amount of dopant. In the leaching solutions of the HF and H_2SO_4/H_3PO_4 experiments no barium can be detected, due to the insolubility of the reaction products. However, the resistance in these media is less than e.g. in concentrated HCl or HNO_3.

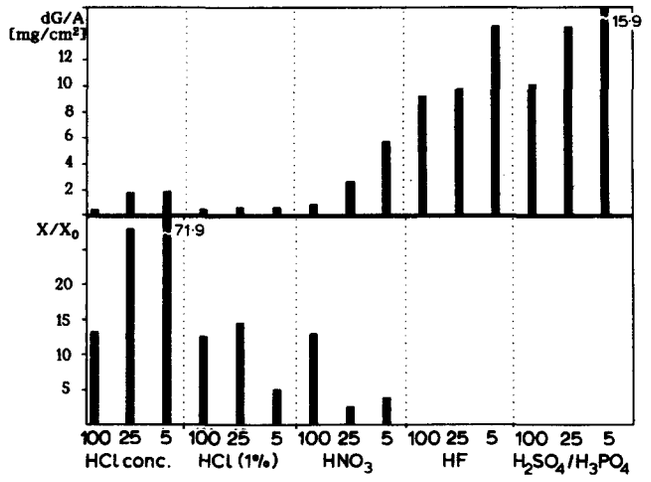

Fig. 10. Specific weight loss and ratio of additive concentration in leaching solutions and bulk materials for BaO-doped alumina. Corrosion results with samples 5 Ba, 25 Ba and 100 Ba in concentrated HCl, HNO_3, HF and H_2SO_4/H_3PO_4 (1:1) at 180°C, 168 h and HCl (1%) at 245°C, 24 h.

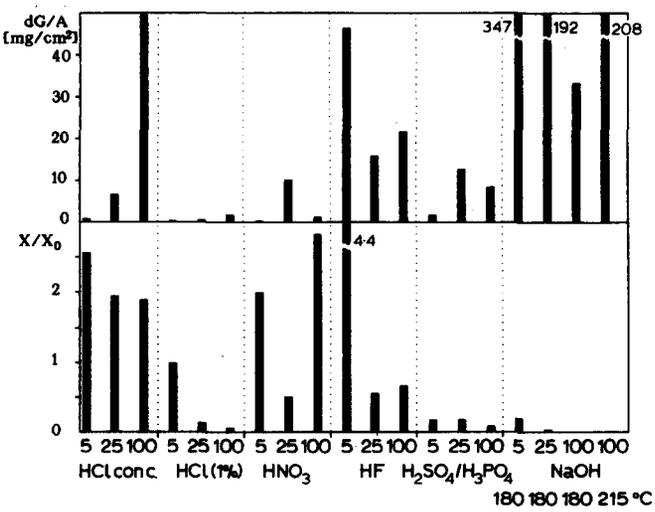

Fig. 11. Specific weight loss and ratio of additive concentrations in leaching solutions and bulk material for ZrO_2-doped alumina. Corrosion results with samples 5 Zr, 25 Zr and 100 Zr in concentrated HCl, HNO_3, HF, H_2SO_4/H_3PO_4 (1:1) and NaOH (10%) at 180°C, 168 h (if not indicated differently) and HCl (1%) at 245°C, 24 h.

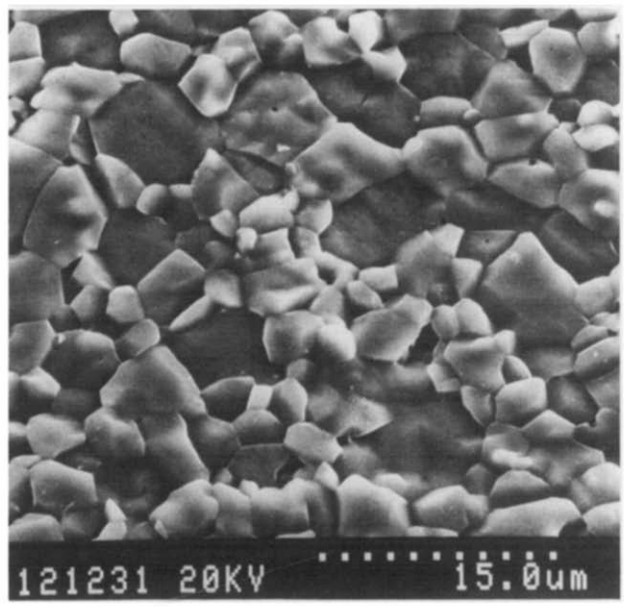

(a)

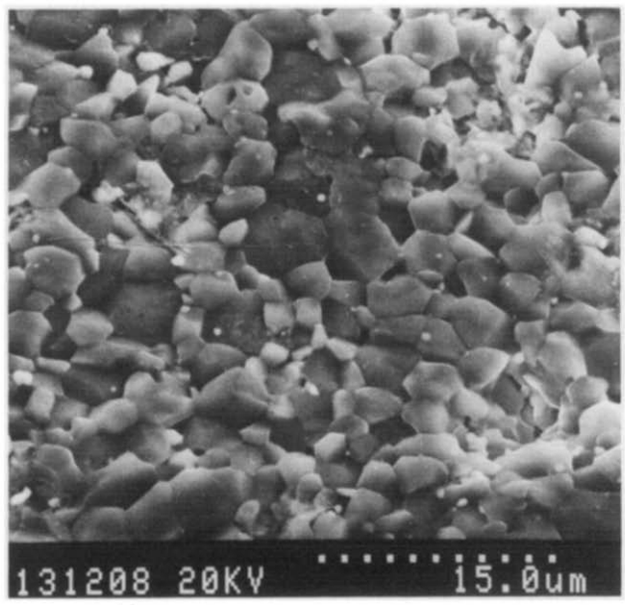

(b)

Fig. 12. SEM micrographs of ZrO_2-doped samples (a) 5 Zr and (b) 100 Zr after a corrosion experiment in HCl (1%, 180°C, 168 h).

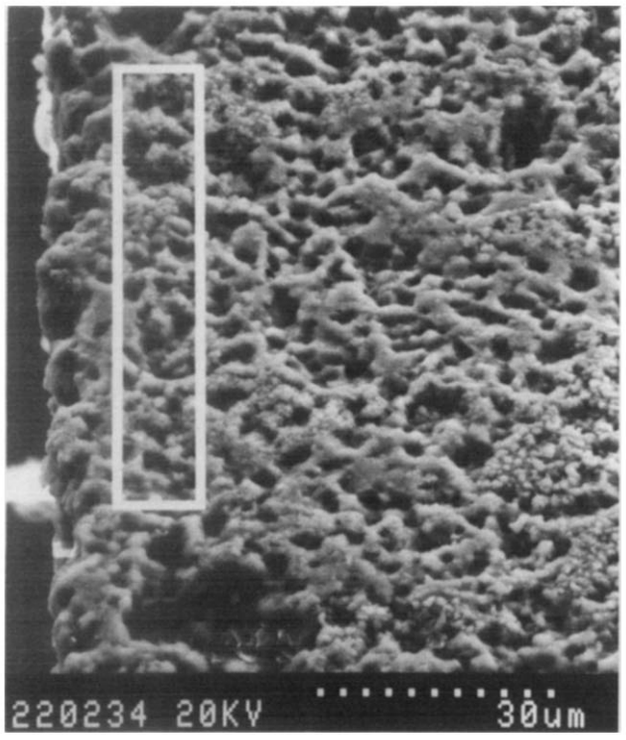

Fig. 13. SEM micrograph of a ZrO_2-doped sample (100 Zr) after a corrosion experiment in NaOH (10%, 180°C, 168 h); area of EDX measurement.

4.4 ZrO_2-Doped alumina

In Fig. 11 the results of the corrosion experiments with zirconium oxide-doped alumina are plotted. Whereas the resistance in concentrated HCl decreases significantly with the amount of dopant, the stability in caustic soda and also in concentrated HF is increased. In Fig. 12 the surfaces of zirconium oxide-doped aluminas after attack with 1% HCl at 245°C for one day are shown. The single grains are attacked only slightly and the micrograph of the cross-section shows a sharp sample edge. A very low relative zirconium concentration is found in the leaching solution.

EDX measurements of a sample of the zirconium oxide-doped alumina with high ZrO_2 concentration (100 Zr) showed a decreasing zirconium concentration at the samples edge in relation to the unreacted center and a considerable amount of sodium. A cross-section of the sample is shown in Fig. 13.

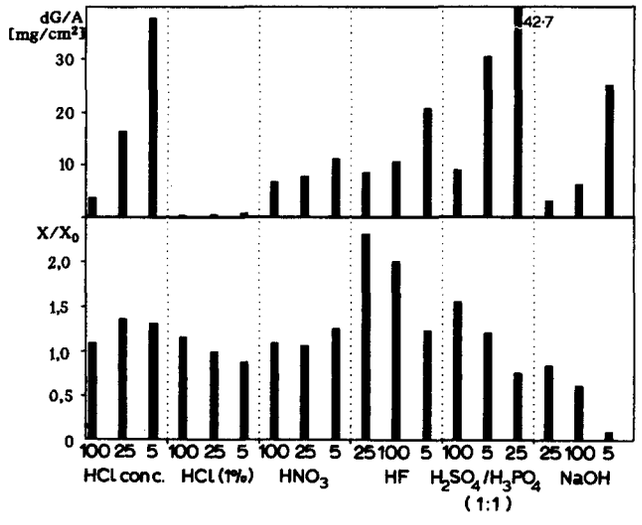

Fig. 14. Specific weight loss and ratio of additive concentration in leaching solutions and bulk material for Cr_2O_3-doped alumina. Corrosion results with samples 5 Cr, 25 Cr and 100 Cr in concentrated HCl, HNO_3, HF, H_2SO_4/H_3PO_4 (1:1) and NaOH (10%) at 180°C, 168 h and HCl (1%) at 245°C, 24 h.

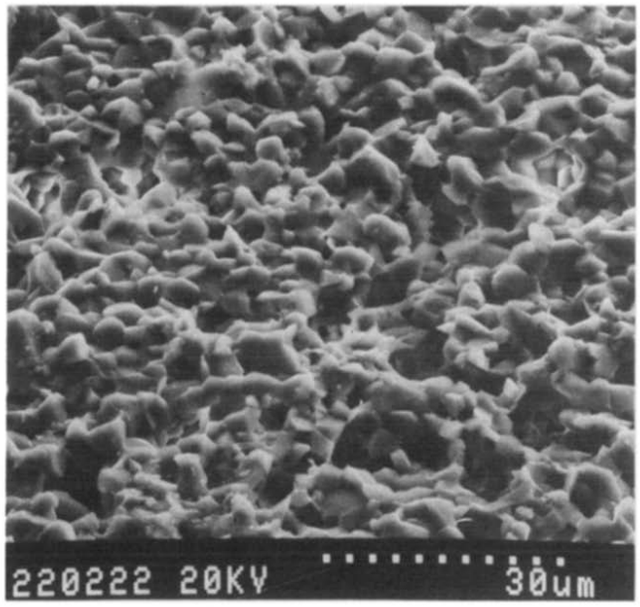

(a)

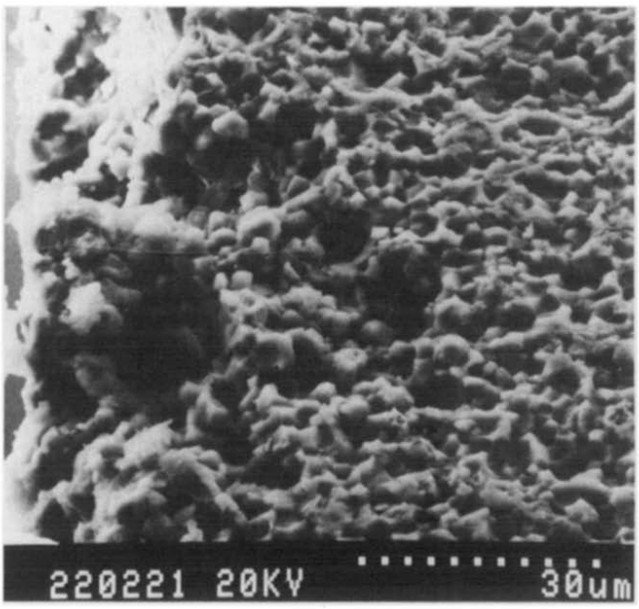

(b)

Fig. 15. SEM micrographs of Cr_2O_3-doped sample (25 Cr) after a corrosion experiment in HCl_{conc} (180°C, 168 h). (a) Surface; (b) cross-section.

4.5 Cr_2O_3-Doped alumina

The high chromium oxide-doped sample 100Cr is relatively stable in caustic soda. At 215°C a weight loss of 34·2 mg/cm^2 has occurred after one week. In contrast to other compositions, the chromium oxide-doped aluminas differ much in their resistance against HCl and HNO_3, as shown in Fig. 14.

In Fig. 15 the SEM of the alumina doped with 2000 μg/g Cr_2O_3 is shown. A relatively strong corrosive attack ($dG/A = 16{\cdot}3$ mg/cm^3) can be observed. In contrast to the silica-doped[6,7] materials no deep penetration into the bulk ceramic has taken place.

Acknowledgement

The authors appreciate the financial support of the Deutsche Forschungsgemeinschaft for this research project.

References

1. Dawihl, W. & Klinger, E., Der Korrosionswiderstand von Aluminiumoxideinkristallen und von gesinterten Werkstoffen auf Aluminiumoxidgrundlage gegen anorganische Säuren. *Ber. DKG*, **44** (1967) 1–4.
2. Ohman, L., Ingri, N. & Tegman, R., Corrosion of dense polycrystalline α-Al_2O_3 in $NaHCO_3$ buffered water solution of pH 8·5 at 40–100°C. *Am. Ceram. Soc. Bull.*, **61** (1982) 567–71.
3. Smailos, E., Schwarzkopf, W., Köster, R. & Storch, W., Untersuchungen zur Eignung keramischer Behälter als Korrosionsschutz für hochradioacktive Abfallprodukte bei der Endlagerung in Steinsalzformationen. Report KfK 4244 (Karlsruhe Nuclear Research Center, Karlsruhe), 1987.
4. Markus, L. O. & Ahrens, R. R., Chemical resistance of solid materials to concentrated phosphoric acid. *Am. Ceram. Soc. Bull.*, **60** (1981) 490–3.
5. Millard, M., Anderson, H. U. & Wuttig, M. W., Influence of grain boundaries on liquid corrosion of Al_2O_3 and NaCl. In *Advances in Ceramics*, ed. M. F. Yan and A. H. Heuer, ACerS 1983, pp. 325–34.
6. Genthe, W. & Hausner, H., Einfluß der Zusammensetzung auf die Korrosion von Aluminiumoxid. Report DFG HA 995/18-1, Berlin, 1988.
7. Genthe, W. & Hausner, H., Korrosionsverhalten von Aluminiumoxid in Säuren und Laugen. *cfi/Ber. DKG*, **67** (1990) 6–11.
8. Genthe, W. & Hausner, H., Corrosion of alumina in acids. In *Euroceramics*, ed. G. de With, R. A. Terpstra, R. Metselaar. Elsevier Applied Science, London, 1989, pp. 3.463–7.
9. Genthe, W., Kadoori-al Robayie, J. & Hausner, H., Korrosion von Zirkonoxid-Werkstoffen. In *Keramik in der Anwendung: Verschleiß und Korrosion*. DKG, Köln, 1990, pp. 305–6.
10. Genthe, W., Kadoori-al Robayie, J. & Hausner, H., Korrosion von SiC/TiC-Werkstoffen in Säuren. *cfi/Ber. DKG* (1991) 262–5.